ARMY RESEARCH LABORATORY

Extinction, Absorption, Scattering, and Backscatter for Aerosolized *Bacillus Subtilis* Var. *Niger* Endospores From 3 to 13 μm

Kristan P. Gurton, David Ligon, and Ramaz Kvavilashvili

ARL-TR-2343 February 2001

The findings in this report are not to be construed as an official Department of the Army position unless so designated by other authorized documents.

Citation of manufacturer's or trade names does not constitute an official endorsement or approval of the use thereof.

Destroy this report when it is no longer needed. Do not return it to the originator.

Army Research Laboratory

Adelphi, MD 20783-1197

ARL-TR-2343 February 2001

Extinction, Absorption, Scattering, and Backscatter for Aerosolized *Bacillus Subtilis* Var. *Niger* Endospores From 3 to 13 μm

Kristan P. Gurton, David Ligon, and Ramaz Kvavilashvili

Computational and Information Sciences Directorate

Abstract

Spectral extinction was measured in situ for aerosolized *Bacillus subtilis* var. *niger* (BG) endospores with the use of Fourier-transform infrared (FTIR) spectroscopy from 3.0 to 13.0 μm. Corresponding aerosol-size distributions were measured with the use of a commercially available elastic light-scattering probe and verified by direct particle capture and subsequent counting via video microscopy. Aerosol mass density was monitored simultaneously with conventional dosimetry and used to mass-normalize the measured spectral extinction. Mie theory calculations based on measured distributions and available complex indices of refraction agreed well. Also present are resultant Mie calculations for the absorption, total scattering, and backscattering. Included are the real and imaginary components of the complex index of refraction for BG as measured by Milham and Quarry. Both calculated and measured cross sections suggest that for wavelengths longer than 6.0 μm, the total extinction is primarily due to absorption. Finally, to offer a comparison, we present measured spectral extinction for three additional aerosols often found in the lower atmosphere, i.e., water fog, diesel soot, and Arizona road dust.

Contents

Figures

1. Introduction

Infrared (IR) spectral extinction for common inorganic aerosols found in the lower atmosphere has been studied and reported on extensively [1–5]. However, research involving the optical properties for intact viruses, fungi, and bacterial aerosols is still extremely rare and woefully lacking [6–8]. Though much of the aggregate bioaerosol material in the lower atmosphere is mundane in nature, reported diseases in humans, animals, and plants have been linked to certain airborne bacteria [9–13]. Tong and Lighthart have reported ambient total atmospheric bacterial (TAB) concentrations for a rural environment that range from 0.1 to 0.001 airborne bacteria per cm^3 ($cells/cm^3$) [14,15].

The ability of one to detect the presence of a harmful bioaerosol from a safe distance is an ever-increasing topic of interest. Proposed optical methods that involve IR light are usually restricted to one or both of the atmospheric transmission window regions, i.e., 3 to 5 μm and/or 8 to 12 μm. These methods usually involve either passive or active illumination schemes, e.g., hyperspectral IR imaging or a CO_2 lidar-type arrangement [16–20]. Whether these (or other) optical techniques are appropriate for the remote detection and identification of harmful bioaerosols remains a topic of discussion. Nevertheless, for the utility of any particular approach to be properly evaluated, certain optical parameters at IR wavelengths for well-characterized bioaerosols are badly needed.

Methods for determining the electromagnetic interaction with bioaerosols usually involve either direct in situ light measurements or particles that exhibit some spherical symmetry (or that are Rayleigh); Mie or a comparable theory may be used to calculate the scattered and absorbed fields. For the latter approach in which the optical interaction is computed, the complex refractive indices for the biomaterials are assumed to be well known. Even when these refractive indices exist (which is rarely), accurate predictive calculations are usually extremely difficult to compute, since these types of particles are typically inhomogeneous and often nonspherical.

We directly measured the IR spectral extinction for aerosolized *Bacillus subtilis* var. *niger* (BG) endospores from 3 to 13 μm using conventional Fourier-transform infrared (FTIR) spectroscopy. Size distributions, aerosol densities, and particle morphology were measured simultaneously. We then compared these results with Mie theory calculations using complex indices of refraction provided by Milham and Quarry [20]. For regions in which there is good agreement between the measured and calculated extinction, we also present the total scatter, absorption, and backscatter components predicted by the Mie theory. Spectral extinction for both bulk powder and thin-film forms of BG is also presented. Finally, we contrast the extinction spectra for BG with three atmospheric aerosols commonly found in the environment, i.e., water fog, diesel soot, and Arizona road dust.

2. Experiment

The BG endospores used in this study were provided by the Edgewood Research Development and Engineering Center (ERDEC), Aberdeen Proving Ground, MD, and were produced in large quantities for use as a biological warfare (BW) simulant. This material, often referred to as "military-grade" BG, was assayed and known to contain 12.7×10^{10} colony-forming units per gram (cfu/g). Ion chromatography was performed on both washed and unwashed suspensions. Results showed small quantities of sulfate ions with lesser amounts of PO_4^{-3}, F^-, and Cl^- ions, which have been attributed to small quantities of residual growth media. Prior ultraviolet fluorescent studies have associated certain anomalous results to these sulfate ions [22]. IR extinction measured here for both washed and unwashed BG samples showed no appreciable differences between the spectra.

The primary transmission measurement was conducted in a 0.5-m^3 aerosol chamber, which provided an optical path length of 0.61 m. Dry and hydrated BG endospores in aerosol form were dispersed separately with a variety of techniques that have proven effective in prior studies. We generated hydrated endospore droplets using two pharmaceutical nebulizers that atomized various concentrations of a BG/water solution. To simulate conditions similar to the open atmosphere, we evaporated the encapsulating water droplets by directing the BG/water spray into a plenum of heated dry air. The resultant spore aerosol was gently drawn into the chamber with a small-area recirculating fan. We continuously monitored relative humidity using a filtered dew-point hygrometer that was inserted through the walls of the chamber.

Dry powdered BG was effectively aerosolized and sprayed into the chamber. Pressurized air was used to inject the endospore powder through a cylindrical nozzle that contained a spiraling array of fine stainless-steel wires. A vortex created within the nozzle effectively separated and dispersed the bacterial spores with minimal agglomeration. Care was taken to properly adjust the air pressure so that spore coatings remained reasonably intact.

We obtained IR transmission spectra using a high-resolution (0.02 wavenumber) Bomem DA2.02 FTIR spectrometer. For this study, the spectrometer was operated in a transmission mode, i.e., spectral attenuation was measured by placing the aerosol chamber between the source and the interferometer. A broadband IR Nernst glower was collimated with a ZnSe condensing lens assembly and projected through the aerosol chamber with two BaF_2 transmission windows that were fitted with dry-air flushes. Transmitted light was coupled to the interferometer with a gold-surfaced f/4 off-axis parabola.

Particle-size distributions were measured with a commercial particle-size spectrometer. We used Particle Measuring Systems, Inc. (PMS), particle spectrometer (model CSASP-100) to monitor in real time the aerosol size distribution. We determined particle-shaped characteristics by analyzing

photographs of captured particles that were collected on shielded glass slides. Using these photographs, we directly counted representative samples and generated a size distribution that agreed well with the distributions measured using the PMS. The resultant size distribution with a corresponding log-normal fit (r modal = 0.89 μm; standard deviation, $\sigma = 0.15$). A typical BG run is shown in figure 1. Photographs also showed that the endospore aerosol consisted of mostly single or minimally agglomerated particles that appeared reasonably spherical (see fig. 2). Aerosol mass densities (g/m^3) were periodically measured by collecting the aerosol on polycarbonate filters while sampling known volumes of air for predetermined periods of time. Results from the dosimetric sampling were then used to mass-normalize the measured extinction (m^2/g).

To offer a comparison, we measured the spectral extinction for three additional "background" aerosols commonly found in the environment, i.e., diesel soot, water fog, and Arizona road dust (SiO_2). Environmental aerosols were generated by either burning diesel fuel (soot), nebulizing distilled water (fog), or dispersing dry dust in a similar manner as just described (Arizona road dust). Spectra were measured and mass-normalized in the same fashion as the BG aerosol.

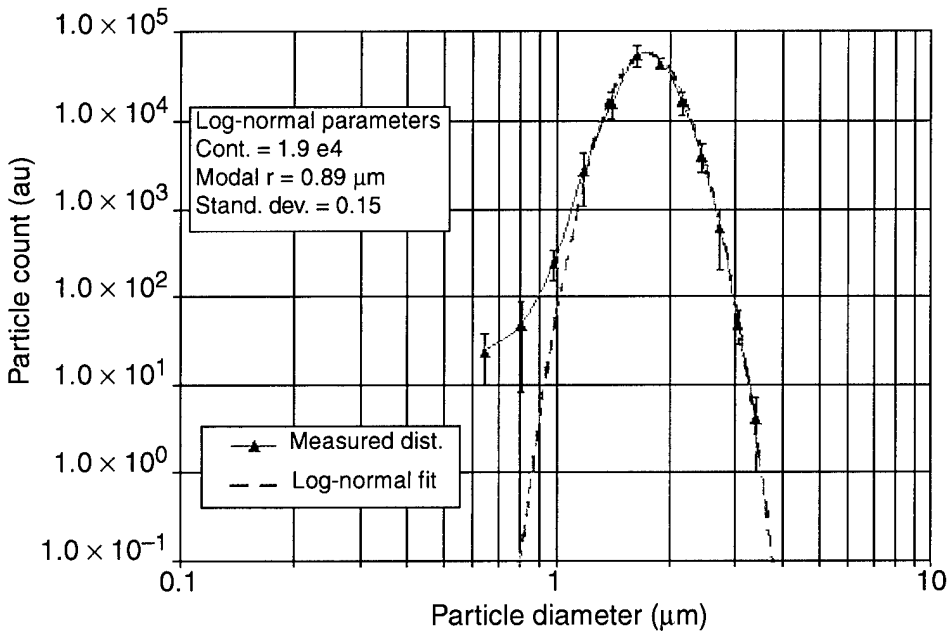

Figure 1. Measured BG size distribution with corresponding log-normal curve fit.

Figure 2. Single BG endospores shown here to be reasonably spherical.

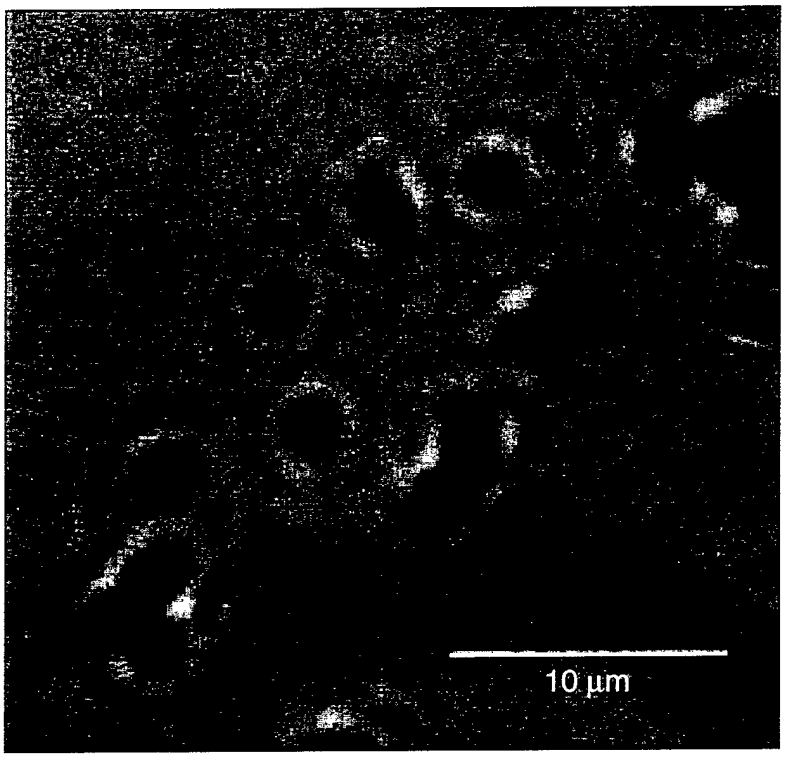

3. Results

Interferograms were recorded before, during, and after each aerosol dispersion. We applied a Bartlet apodization to each interferogram before performing background rationing. Forward-scattering corrections were applied to the raw transmission and were found to be insignificant at the wavelengths above 6 μm. As the wavelength becomes comparable (or smaller) to the endospore diameter, the forward-scattering correction increases monotonically and was found to be as much as 9 percent at 3 μm [23]. Figure 3 shows a typical graph of the recorded transmittance from 3 to 13 μm for a series of concentrations of BG aerosol. Transmission was converted to extinction with a Beer's law relation. Results were mass-normalized by dividing the raw extinction (1/m) by the corresponding aerosol mass density (g/m^3) measured during the dosimetric portion of the experiment (see fig. 4).

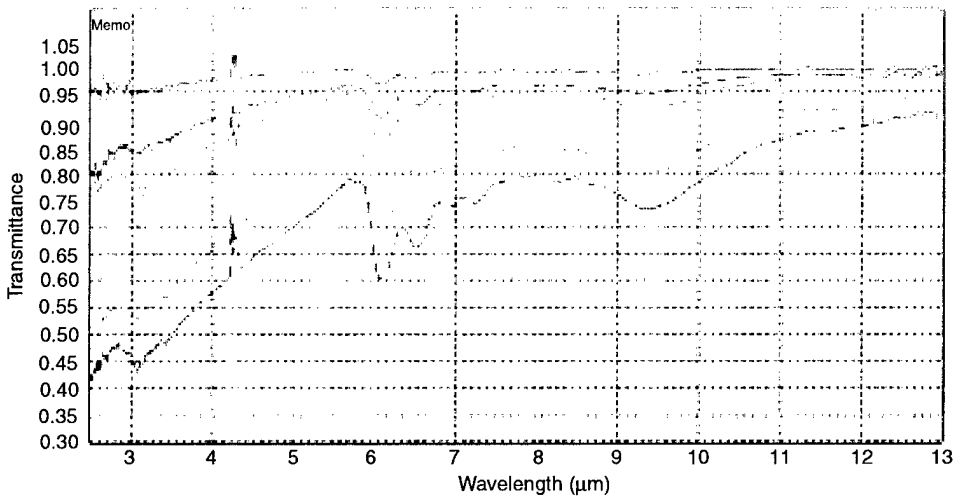

Figure 3. FTIR transmittance for various aerosol concentrations of BG.

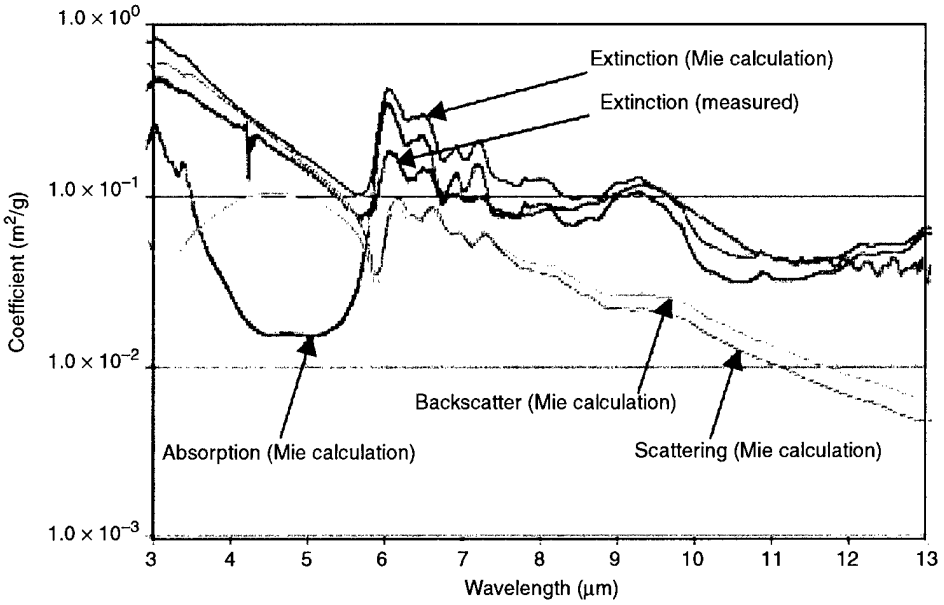

Figure 4. Measured and calculated mass-normalized (m^2/g) extinction, absorption, total scatter, and backscatter cross sections for aerosolized BG endospores.

Figure 4 shows both measured and calculated cross sections. Mie theory cross sections were calculated by convolving the measured size distribution with the complex indices of refraction (provided by Milham and Quarry) shown in figure 5 [20]. As one can see, the measured extinction shows similar form to the calculated spectra, albeit at slightly reduced levels. What is interesting and worth noting is that beyond 6 μm, the Mie calculations show that almost all the extinction for the BG aerosol is due to absorption.

Particle number densities were calculated by integrating the measured size distribution with the estimated mass per particle (bulk density for BG taken to be 1.45 g/cm^3) and equating it to the measured aerosol mass density [25]. Particle number densities for a typical run ranged from a low of 2×10^3 endospores/cm^3 for periods in which a significant amount of settling had occurred to peak values on the order of 1×10^6 endospores/cm^3 for periods shortly after the initial dispersion. Note that certain spectral features became difficult to resolve when particle number densities fell much below 10^3 endospores/cm^3 (based on our relatively small 0.61-m path length).

It is sometimes convenient to represent the coefficients shown in figure 4 on a "per-spore" basis. Using the measured size distribution and assuming the endospores and their agglomerates are reasonably spherical, we calculate a value of approximately 5×10^{-12} g/spore, which can then be used to convert the mass-normalized quantities shown in figure 4 (m^2/g) to cross sections per spore (m^2/spore). As an example, we find from figure 4 the mass-normalized extinction at 9.32 μm to be 1.16×10^{-1} m^2/g. Multiplying this value by the conversion factor, 5×10^{-12} g/spore, we calculate the extinction cross section per spore to be 0.583×10^{-12} m^2/spore. This compares well with the Mie theory calculated value of 0.525×10^{-12} m^2/spore.

To contrast these results, we measured the extinction spectra for three atmospheric aerosols, i.e., water fog, diesel soot, and Arizona road dust. A similar set of measurements was repeated for the three environmental aerosols. Care was taken to ensure that generated size distributions (especially for the water fog) were similar to those measured in the field [26]. Mass-normalized extinction spectra for the three aerosols are compared with BG and are shown in figure 6. Absorption caused by residual water vapor produced the fine structure seen between 5 and 8 μm in both the fog and soot spectra, and the apparent spike seen near 4.25 μm in all spectra (especially for soot) was identified as residual CO_2.

Figure 5. (a) Real and (b) imaginary indices of refraction for BG.

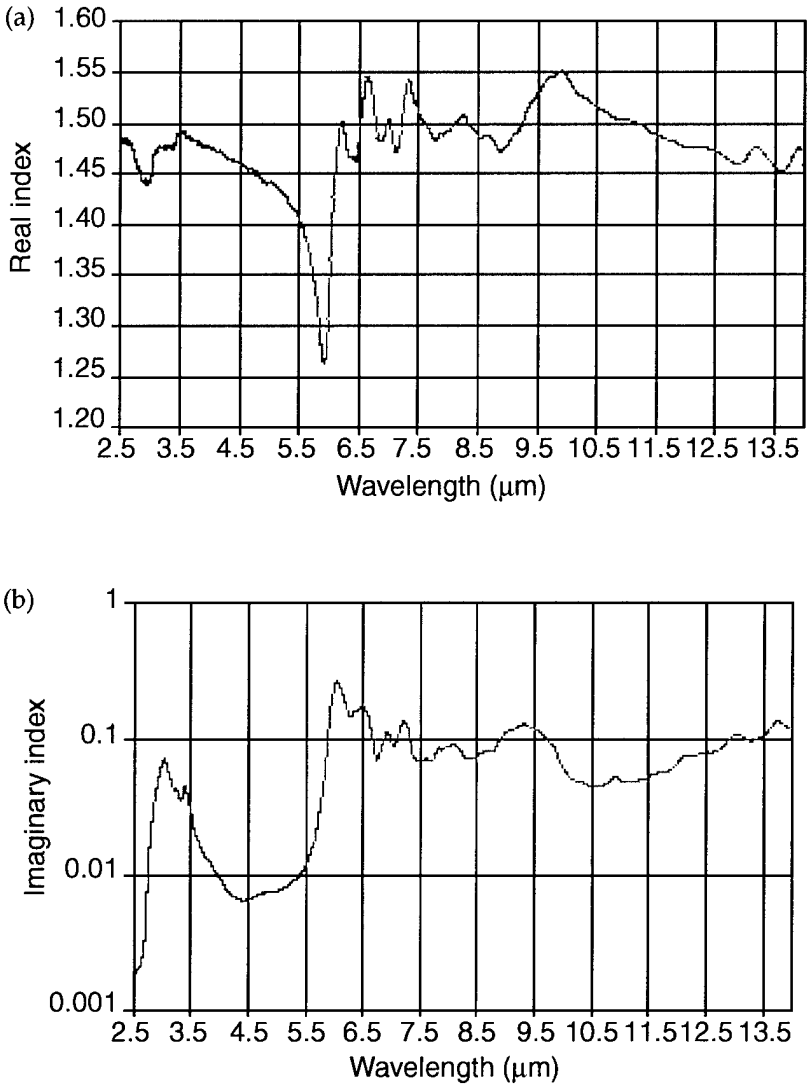

Figure 6. Comparison of measured mass-normalized extinction (m^2/g) for BG with three common background aerosols, i.e., water fog, Arizona road dust, and diesel soot.

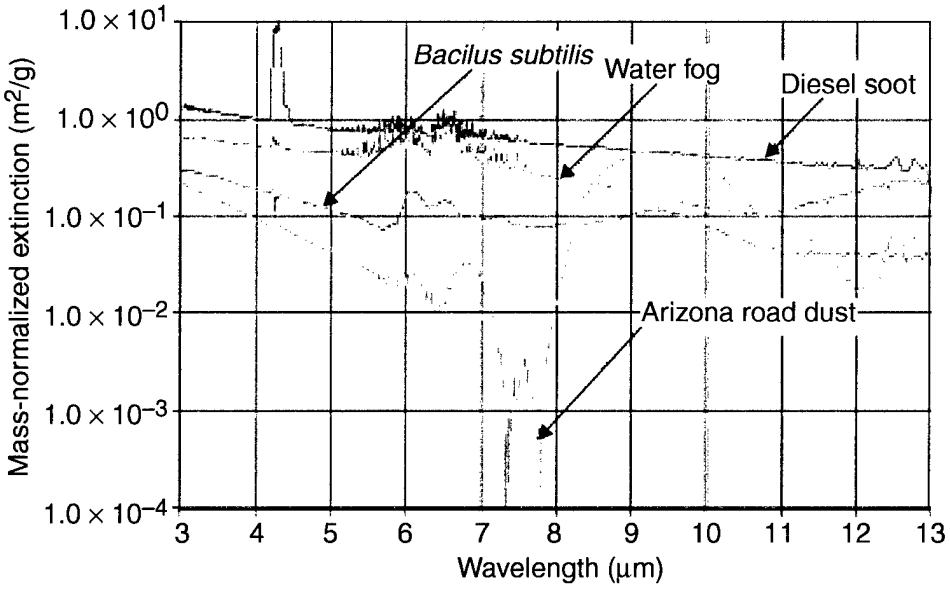

4. Discussion

As seen in figure 6, BG shows relatively moderate extinction at the IR wavelengths considered (on a mass-normalized basis) when compared to the various background aerosols. As expected, the spectra for aerosolized BG are relatively smooth and devoid of any sharp identifiable "line" structure. While many of the IR bands of intact microorganisms still have to be assigned unambiguously, preliminary species identification conducted on biological thin-films has been reported [27].

The most characteristic features associated with the presence of certain spore proteins occur in the range between 5.6 and 6.6 μm and are attributed to the so-called "amide I and II" absorption bands. Unfortunately, this highly characteristic region lies in the middle of the most opaque portion of the atmosphere and is probably of little value when possible remote detection techniques are considered (i.e., because of strong water vapor absorption, transmission from 5 to 8 μm is nearly impossible) [28]. Naumann and Helm have tentatively identified the smooth broadly peaked region between 8 and 11 μm as a superposition of many fine absorption bands caused by C-O-C and C-O-P stretching of predominantly polysaccharide or phophodiester [29]. Naumann and Helm assert that the peak around 9.3 mm is due primarily to symmetric molecular vibrations of phosphate diesters. Beyond 11 μm, the region exhibits a variety of weak but extremely characteristic features attributed to aromatic ring vibrations of phenylalanine, tyrosine, tryptophan, and various nucleotides. With the exception of a few weak peaks around 13 μm (resulting from $>CH_2$ rocking modes of fatty acid chains), specific assignment is impossible. Although this region appears relatively featureless, Naumann and Helm have successfully used this 8- to 13-μm region for taxonomical identification of bacterial thin-films. Because of this, the region is often referred to as the "bacterial fingerprint region."

Because much of the existing information (albeit limited) involving IR spectra for biological materials is derived from thin-film samples, we thought it interesting to compare differences among extinction spectra for various forms of BG. Figure 7 shows a comparison of the spectral extinction for aerosolized BG, bulk powdered BG (measured with attenuated total reflection (ATR)), and thin-film spectra taken from Yabushita and Wada [27]. As expected, much of the spectral information is similar from one form to another for regions where absorption is predicted to dominate. Also seen in figure 7 are the effects caused by scattering. As the ratio of the spore diameter to wavelength becomes larger, scattering begins to dominate in the aerosol extinction. Certain absorption features seen near 3 μm for the bulk and thin-film spectra are completely obscured by particulate scattering and are not seen in the aerosol spectra.

As one can see in figures 4, 6, and 7, most aerosol spectra tend to be devoid of any easily identifiable characteristic features. This makes reliable identification difficult with the use of conventional spectra correlation techniques. Naumann and Helm have demonstrated the ability to rapidly classify and

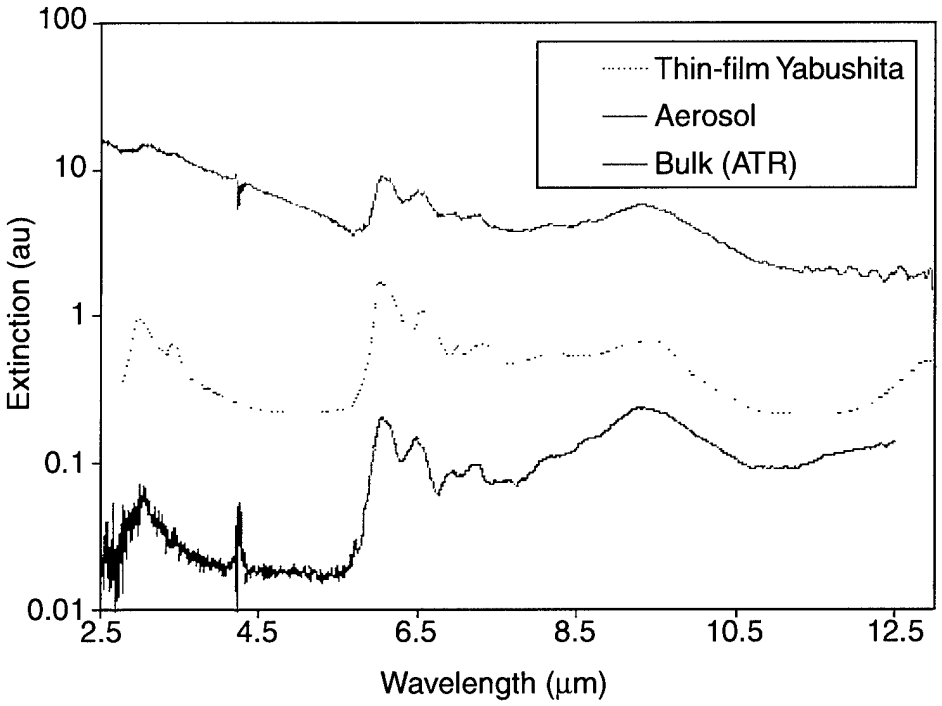

Figure 7. Comparison of FTIR measurements conducted on various forms of BG, i.e., aerosolized BG (top), thin-film slurry (middle), and bulk powdered BG (bottom).

group intact bacterial specimens using a technique called "cluster analysis" [6]. Their approach is based on treating spectra as images or patterns and applying classic pattern recognition algorithms to discriminate subtle differences among similar spectra. A variety of simple mathematical operations is applied to weighted wavelength regions based on certain predetermined criteria. In addition, when comparing one spectral form to another, one must consider carefully how the aerosol spectra were recorded. Bryson and Flanigan have reported on an obvious but interesting effect witnessed during a series of FTIR aerosol field measurements [28]. They report that for wavelengths in which aerosols are highly absorbing, as is for BG above 6 μm, measured transmission may appear as either an extinction or *emission* spectra (one being the mirror image of the other), depending on whether the background is considered hot or cold relative to the aerosol. The symmetry relation between absorption and emission spectra is a direct result of Kirchhoff's law that relates aerosol absorption efficiencies to particle emissivity [29]. Under such conditions, it would be desirable to consider a "form"-preserving operation that is independent of aerosol density and/or background conditions.

As an example, we apply two simple form-preserving operations on the measured extinction spectra, i.e., first and second derivatives (see fig. 8). Figure 8 shows the original extinction for each aerosol measured at various concentrations (top spectra in each frame). Below each extinction curve, we show the resultant first and second derivatives. One fairly easy parameter to "key on" would be the spectral position of where the first and second derivatives cross zero (shaded narrow regions). Minor variance in defining these zeros arises when attenuation is extremely weak because of low aerosol concentrations.

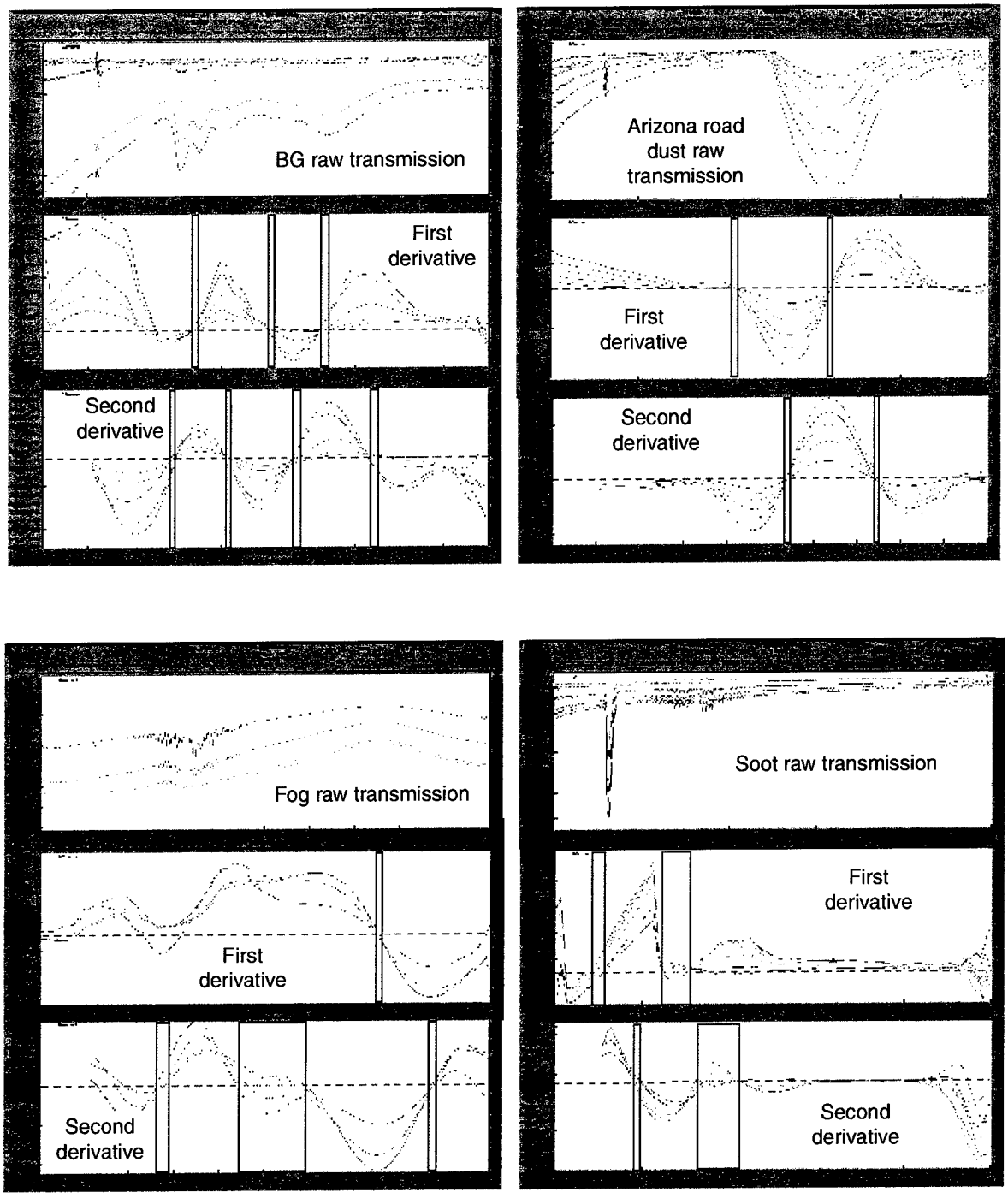

Figure 8. Example of two simple "form-preserving" operations (i.e., first and second derivatives) that one might consider to discriminate subtle differences among similar spectra. Each set of three frames consists of original transmission spectra measured for various aerosol densities (top) and corresponding first (middle) and second (bottom) derivatives.

The question remains: "Can one remotely identify the presence of a harmful bioaerosol using conventional IR transmission measurements like those conducted here?" The answer to this question is complex and a function of many parameters, e.g., optical depth, sensor response, ambient atmospheric conditions, etc. As a result, we make no attempt to give a definitive answer. However, certain key aspects should be addressed when considering such a scenario.

First, because aerosol extinction spectra have a tendency to be relatively smooth, low-resolution spectroscopy will usually suffice. Although the spectrometer used for this study was set at a resolving power of 4 cm^{-1}, no spectral features were observed that could not be resolved at a substantially lower setting, for example, 20 cm^{-1}. Second, a reasonable amount of bioaerosol material must obviously be present (relative to ambient conditions) to discern noticeable changes in the transmission.

To get an "order of magnitude" estimate of the bioaerosol concentrations necessary to be spectroscopically measurable, let us first assume a simple transmisometer-type arrangement in which a homogenous bioaerosol cloud obscures a sufficiently powerful broadband IR source. Assuming an endospore cloud 100 m in extent obscures a similarly dimensioned optical path for a collimated beam (diameter 4 cm), we estimate a minimum detectable particle density (to achieve a reasonable amount of attenuation) to be on the order of 10 to 20 particles/cm^3.

Up to this point, we have assumed that clear conditions and effects caused by the intervening atmosphere were negligible, i.e., spectral masking because of path radiance and molecular absorption by gaseous CO_2, H_2O, and O_3. When these effects are considered and the distance from the spectrometer to the biocloud is in excess of 5 km or more, the minimum detection limits stated in the previous paragraph increase several fold. This seems to restrict the type of approach one might consider to the "plume identification" realm in which the measurement is conducted near to the source and that the bioaerosol cloud is sufficiently dense. Based on this and our experience in measuring aerosol spectra, we believe that the remote detection of a bioaerosol using IR extinction spectra will be limited to active illumination techniques in which the source of radiation is sufficiently strong enough to overcome the detrimental effects caused by atmospheric absorption and path/ground radiance.

Acknowledgments

We would like to thank William Loerop and Dorothea Paterno (ERDEC, Aberdeen Proving Ground, MD) for providing their expertise and the bioaerosol materials necessary for this study. We would also like to thank Dennis Flanigan (also with ERDEC) for an enlightening conversation on this topic.

References

1. H. C. Van De Hulst, *Light Scattering by Small Particles*, John Wiley and Sons, New York (1989).
2. C. F. Bohren and D. R. Huffman, *Absorption and Scattering of Light by Small Particles*, John Wiley and Sons, New York (1983).
3. M. Kerker, *The Scattering of Light and Other Electromagnetic Radiation*, Academic Press, Inc., New York (1969).
4. H. E. Gerber and E. E. Hindman, *Light Absorption by Aerosol Particles*, Spectrum Press, Hampton, VA (1982).
5. A. Deepak, *Atmospheric Aerosols*, Spectrum Press, Hampton, VA (1982).
6. D. Helm and D. Naumann, "Identification of some bacterial cell components by FTIR spectroscopy," *FEMS Microbiol. Lett.* **126**, 75–80 (1995).
7. D. B. Hedrick, D. E. Nivens, and C. Stafford, "Rapid differentiation of archaebacteria from eubacteria by diffuse reflectance Fourier-transform IR spectroscopic analysis," *J. Microbiol. Methods* **13**, 67–73 (1991).
8. H. H. Mantsch and D. Chapman, *Infrared Spectroscopy of Biomolecules*, Wiley-Liss, New York (1996).
9. B. Lighthart and G. Mohr, *Atmos. Microbiol. Aerosols*, Chapman-Hall, New York (1994).
10. T. Madelin, "Fungal aerosols—A review," *J. Aerosol Sci.* **25**, 1405–1412 (1994).
11. F. M. Racine and J. C. Vary, "Isolation and properties of membranes from *Bacillus megaterium* spores," *J. Bacteriol.* **143**, 1208–1214 (1980).
12. S. Matthias-Maser and R. Jaenick, "Examination of atmospheric bioaerosols particles with radii greater than 0.2 micrometer," *J. Aerosol Sci.* **25**, 1605–1613 (1994).
13. P. S. Tuminello and E. T. Arakawa, "Optical properties of *Bacillus subtilis* spores from 0.2 to 2.5 μm," *Appl. Opt.* **36**, No.13 (1997).
14. Y. Tong and B. Lighthart, "Diurnal distribution of total and culturable atmospheric bacteria at a rural site," *Aerosol Sci. Technol.* **30**, 246–254 (1999).
15. Y. Tong and B. Lighthart, "The annual bacterial particle concentration and size distribution in the ambient atmosphere in a rural area of the Willamette Valley, Oregon," *Aerosol Sci. Technol.* **32**, 393–403 (2000).
16. D. F. Flanigan, "Hazardous cloud imaging: A new way of using passive infrared," *Appl. Opt.* **36**, No. 27, 7027–7036 (1997).
17. W. B. Grant, "LIDAR for atmospheric and hydrospheric studies," in *Tunable Laser Applications*, F. J. Duarte, ed., Marcel Dekker, New York (1995).
18. R. M. Measures, *Laser Remote Sensing*, John Wiley and Sons, New York (1984).

19. J. P. Carrico, "The DOD chemical-biological stand-off detection program: A revisit nearly ten years later," *Third Workshop on Stand-off Detection for Chemical and Biological Defense*, Williamsburg, VA (17–21 October 1994).

20. D. F. Flanigan, *Hazardous Cloud Imaging: An In-Depth Study*, Technical Report ERDEC-TR-416, Appendix B, Edgewood Research Development and Engineering Center (ERDEC), Aberdeen Proving Grounds, MD (1997).

21. P. M. Pellegrino and N. F. Fell, "Bacterial endospore detection using terbium dipicolinate photoluminescence in the presence of chemical and biological materials," *Anal. Chem.* **70**, 1755–1760 (1998).

22. A. Deepak and M. Box, "Forward scattering correction for optical extinction measurements in aerosol media. 2: Polydispersions," *Appl. Opt.* **17**, No. 19, 3169–3176 (1978).

23. G. W. Faris, R. Copeland, K. Mortelmans, and B. Bronk, "Spectrally resolved absolute fluorescence cross sections for bacillus spores," *Appl. Opt.* **36**, No. 4, 958–967 (1997).

24. E. Shettle and R. Fenn, *Models for the Aerosols of the Lower Atmosphere and the Effects of Humidity Variations on Their Optical Properties*, Air Force Geophysics Laboratory, Technical Report AFGL-TR-79-0214 (September 1979).

25. H. Weichel, *Laser Beam Propagation in the Atmosphere*, SPIE Optical Engineering Press, Bellingham, WA (1989).

26. D. Naumann and D. Helm, "Microbiological Characterization by FTIR Spectroscopy," *Nature* **351**, 81–82 (1991).

27. S. Yabushita and K. Wada, "A spectroscopic study of the microorganism model of interstellar grains," *Astrophysics Space Sci.* **124**, 377–388 (1986).

28. J. R. Bryson and M. J. Flanagan, "The infrared characterization of smoke and obscurants utilizing the Honeywell background measurement spectroradiometer," *Proc. Smoke/Obscurants Symposium V*, OPM Technical Report DRCPM-SMK-T-001-81, 241–274 (April 1981).

29. G. W. Kattawar and M. Eisner, "Radiation from a homogenous isothermal sphere," *Appl. Opt.* **9**, 2685–2690 (1970).

Distribution

Admnstr
Defns Techl Info Ctr
ATTN DTIC-OCP
8725 John J Kingman Rd Ste 0944
FT Belvoir VA 22060-6218

DARPA
ATTN S Welby
3701 N Fairfax Dr
Arlington VA 22203-1714

Ofc of the Secy of Defns
ATTN ODDRE (R&AT)
The Pentagon
Washington DC 20301-3080

Ofc of the Secy of Defns
ATTN OUSD(A&T)/ODDR&E(R) R J Trew
3080 Defense Pentagon
Washington DC 20301-7100

AMCOM MRDEC
ATTN AMSMI-RD W C McCorkle
Redstone Arsenal AL 35898-5240

ARL Chemical Biology Nuc Effects Div
ATTN AMSRL-SL-CO
Aberdeen Proving Ground MD 21005-5423

Army Corps of Engrs
Engr Topographics Lab
ATTN CETEC-TR-G P F Krause
7701 Telegraph Rd
Alexandria VA 22315-3864

Army Field Artillery Schl
ATTN ATSF-TSM-TA
FT Sill OK 73503-5000

Army Infantry
ATTN ATSH-CD-CS-OR E Dutoit
FT Benning GA 30905-5090

US Army TRADOC
Battle Lab Integration & Techl Dirctrt
ATTN ATCD-B
FT Monroe VA 23651-5850

Dept of the Army
Assist Secy of the Army
ATTN SAAL-TT L Stotts
2511 Jefferson Davis Hw Ste 9800
Arlington VA 22202-3911

US Military Acdmy
Mathematical Sci Ctr of Excellence
ATTN MADN-MATH MAJ M Huber
Thayer Hall
West Point NY 10996-1786

Natl Ground Intllgnc Ctr
Army Foreign Sci Tech Ctr
ATTN CM
220 7th Stret NE
Charlottesville VA 22901-5396

Natl Security Agcy
ATTN W21 Longbothum
9800 Savage Rd
FT George G Meade MD 20755-6000

Dir for MANPRINT
Ofc of the Deputy Chief of Staff for Prsnnl
ATTN J Hiller
The Pentagon Rm 2C733
Washington DC 20301-0300

SMC/CZA
2435 Vela Way Ste 1613
El Segundo CA 90245-5500

TECOM
ATTN AMSTE-CL
Aberdeen Proving Ground MD 21005-5057

US Army ARDEC
ATTN AMSTA-AR-TD
Bldg 1
Picatinny Arsenal NJ 07806-5000

US Army Info Sys Engrg Cmnd
ATTN AMSEL-IE-TD F Jenia
FT Huachuca AZ 85613-5300

Distribution (cont'd)

US Army Natick RDEC
Acting Techl Dir
ATTN SBCN-T P Brandler
Natick MA 01760-5002

US Army Simulation Train & Instrmntn Cmnd
ATTN AMSTI-CG M Macedonia
ATTN J Stahl
12350 Research Parkway
Orlando FL 32826-3726

US Army Tank-Automtv Cmnd RDEC
ATTN AMSTA-TR J Chapin
Warren MI 48397-5000

US Army Topo Engrg Ctr
ATTN CETEC-ZC
FT Belvoir VA 22060-5546

US Army TRADOC
ATTN ATRC-WEC D Dixon
White Sands Missile Range NM 88002-5501

US Army TRADOC
ATTN ATCD-FA
FT Monroe VA 23651-5170

Nav Air War Ctr Wpn Div
ATTN CMD 420000D C0245 A Shlanta
1 Admin Cir
China Lake CA 93555-6001

Nav Surfc Warfare Ctr
ATTN Code B07 J Pennella
17320 Dahlgren Rd Bldg 1470 Rm 1101
Dahlgren VA 22448-5100

Nav Surfc Weapons Ctr
ATTN Code G63
Dahlgren VA 22448-5000

AF Rsrch Lab Phillips Lab Atmos Sci Div Geophysics Dirctrt
Hanscom AFB MA 01731-5000

AFSPC/DRFN
ATTN CAPT R Koon
150 Vandenberg Stret Ste 1105
Peterson AFB CO 80914-45900

ASC OL/YUH
ATTN JDAM-PIP LT V Jolley
102 W D Ave
Eglin AFB FL 32542

Directed Energy Dirctrt
ATTN AFRL-DEBA
3550 Aberden Ave SE
Kirtland AFB NM 87117-5776

Phillips Lab Atmos Sci Div
Geophysics Dirctrt
ATTN PL-LYP Chisholm
Kirtland AFB NM 87118-6008

USAF Rome Lab Tech
ATTN Corridor W Ste 262 RL SUL
26 Electr Pkwy Bldg 106
Griffiss AFB NY 13441-4514

NASA Marshal Spc Flt Ctr
Atmos Sci Div
ATTN Code ED 41 1
Huntsville AL 35812

NIST
ATTN MS 847.5 M Weiss
325 Broadway
Boulder CO 80303

BD Systems
ATTN J Butts
385 Van Ness Ave #200
Torrance CA 90501

Hicks & Assoc Inc
ATTN G Singley III
1710 Goodrich Dr Ste 1300
McLean VA 22102

Distribution (cont'd)

Natl Ctr for Atmos Rsrch
ATTN NCAR Library Serials
PO Box 3000
Boulder CO 80307-3000

Director
US Army Rsrch Ofc
ATTN AMSRL-RO-D JCI Chang
ATTN AMSRL-RO-EN W D Bach
ATTN AMXRO-GS
PO Box 12211
Research Triangle Park NC 27709

US Army Rsrch Lab
ATTN AMSRL-D D R Smith
ATTN AMSRL-DD J M Miller
ATTN AMSRL-CI-AI-R Mail & Records Mgmt
ATTN AMSRL-CI-AP Techl Pub (2 copies)
ATTN AMSRL-CI-LL Techl Lib (2 copies)
ATTN AMSRL-CI-EP K P Gurton (20)
ATTN AMSRL-CI-EP D Ligon (10 copies)
ATTN AMSRL-CI-EP R Kvavilashvili
Adelphi MD 20783-1197

REPORT DOCUMENTATION PAGE

Form Approved
OMB No. 0704-0188

1. AGENCY USE ONLY *(Leave blank)*	2. REPORT DATE	3. REPORT TYPE AND DATES COVERED
	February 2001	Final, 1 Aug 1999 to 1 Aug 2000

4. TITLE AND SUBTITLE Extinction, Absorption, Scattering, and Backscatter for Aerosolized *Bacillus Subtilis* Var. *Niger* Endospores From 3 to 13 μm

5. FUNDING NUMBERS
DA PR: B53A
PE: 61102A

6. AUTHOR(S) Kristan P. Gurton, David Ligon, and Ramaz Kvavilashvili

7. PERFORMING ORGANIZATION NAME(S) AND ADDRESS(ES)
U.S. Army Research Laboratory
Attn: AMSRL-CI-EP email: kgurton@arl.army.mil
2800 Powder Mill Road
Adelphi, MD 20783-1197

8. PERFORMING ORGANIZATION REPORT NUMBER
ARL-TR-2343

9. SPONSORING/MONITORING AGENCY NAME(S) AND ADDRESS(ES)
U.S. Army Research Laboratory
2800 Powder Mill Road
Adelphi, MD 20783-1197

10. SPONSORING/MONITORING AGENCY REPORT NUMBER

11. SUPPLEMENTARY NOTES
ARL PR: 0FEJ60
AMS code: 61110253A11

12a. DISTRIBUTION/AVAILABILITY STATEMENT Approved for public release; distribution unlimited.

12b. DISTRIBUTION CODE

13. ABSTRACT *(Maximum 200 words)*

Spectral extinction was measured in situ for aerosolized *Bacillus subtilis* var. *niger* (BG) endospores with the use of Fourier-transform infrared (FTIR) spectroscopy from 3.0 to 13.0 μm. Corresponding aerosol-size distributions were measured with the use of a commercially available elastic light-scattering probe and verified by direct particle capture and subsequent counting via video microscopy. Aerosol mass density was monitored simultaneously with conventional dosimetry and used to mass-normalize the measured spectral extinction. Mie theory calculations based on measured distributions and available complex indices of refraction agreed well. Also present are resultant Mie calculations for the absorption, total scattering, and backscattering. Included are the real and imaginary components of the complex index of refraction for BG as measured by Milham and Quarry. Both calculated and measured cross sections suggest that for wavelengths longer than 6.0 μm, the total extinction is primarily due to absorption. Finally, to offer a comparison, we present measured spectral extinction for three additional aerosols often found in the lower atmosphere, i.e., water fog, diesel soot, and Arizona road dust.

14. SUBJECT TERMS	15. NUMBER OF PAGES
Bioaerosol, infrared extinction, aerosol	23
	16. PRICE CODE

17. SECURITY CLASSIFICATION OF REPORT	18. SECURITY CLASSIFICATION OF THIS PAGE	19. SECURITY CLASSIFICATION OF ABSTRACT	20. LIMITATION OF ABSTRACT
Unclassified	Unclassified	Unclassified	UL

NSN 7540-01-280-5500

Standard Form 298 (Rev. 2-89)
Prescribed by ANSI Std. Z39-18
298-102